RAPID COMMUNICATIONS

PHYSICAL REVIEW B VOLUME 47, NUMBER 11 15 MARCH 1993-I

Prevention of crystallization by surfactants during Si molecular-beam deposition on amorphous-Si films

Akira Sakai, Toru Tatsumi, and Koichi Ishida
Microelectronics Research Laboratories, NEC Corporation, 34 Miyukigaoka, Tsukuba, Ibaraki 305, Japan
(Received 17 December 1992)

We have investigated the effect of Sb surfactants on the crystallization of Si adatoms on the amorphous-Si (*a*-Si) surface during Si molecular-beam deposition. It was observed that the Sb segregated to the surface and prevented crystallization, resulting in *a*-Si formation even at around 600 °C. Comparison of the grain growth modes on the *a*-Si surface with and without the surfactant clearly shows the reduction of the diffusion length of the surface-free adatoms by the surfactant.

In various deposition methods, the crystallographic structure of deposited thin films is determined by many factors in both the substrates and the deposited materials. For example, atomic ordering on the substrate surface, lattice mismatch, surface and interface free energies, substrate temperature, chemical bonding, etc., all influence the structure. It was recently shown that the introduction of a small amount of a group-V element as a surfactant during molecular-beam epitaxy (MBE) drastically altered the resultant microstructure of the films.[1–9] This has been demonstrated primarily in Ge-Si systems with As or Sb surfactants. The phenomena have been explained by the energetics of surfactant termination of the substrate and deposited film surfaces. Strong reduction of the free energies of both surfaces by the surfactant gives rise to rapid incorporation of the deposited atoms into subsurface sites, resulting in a change of the growth mode from island to layer-by-layer growth.[3–6] Recently, an atomistic mechanism of surfactant-mediated epitaxial growth has also been proposed.[10]

In the case of deposition onto amorphous substrates, the crystallographic structure of the deposited film strongly depends on the substrate temperature during deposition since the substrate itself has no long-range-ordered structure. Room-temperature Si molecular-beam deposition (Si-MBD) on a SiO_2 substrate under ultrahigh vacuum (UHV) conditions is a well-known procedure for producing amorphous-Si (*a*-Si) films.[11,12] At an elevated substrate temperature of typically about 500 °C, the deposited film has a polycrystalline texture.[13] This structure is explained in terms of random nucleation of deposited Si adatoms on the SiO_2 surface and growth of the nuclei into larger grains. This type of crystallization of Si adatoms also occurs on *a*-Si substrates having clean, native oxide-free surfaces; Si microcrystals have been formed by Si-MBD onto an *a*-Si surface at medium substrate temperatures of 450–650 °C.[14]

In this paper, we demonstrate surfactant-mediated Si-MBD on *a*-Si substrates under UHV conditions. We show that Sb adsorbed on the *a*-Si surface prevents crystallization of Si adatoms on that surface even at medium substrate temperatures.

The experiments were carried out using UHV-MBE equipment with a base pressure of 1×10^{-10} Torr. The Si source was an electron beam evaporator (8 kV), and Sb was evaporated from a boron nitride Knudsen cell. A 100-Å-thick *a*-Si layer was prepared by room-temperature Si-MBD on top of the native oxide layer of a Si(001) substrate. The pressure rose to no more than 10^{-8} Torr during deposition. Then the *a*-Si surface with or without the adsorbed Sb was exposed to a Si molecular beam of flux density 3.5×10^{14} atoms/cm^2 s for a certain period at a temperature in the range 450–650 °C. The concentration of Sb adsorbed on the surface was measured by the peak height ratios of Si and Sb in *in situ* Auger electron spectroscopy (AES). A deposited amount of Sb on the *a*-Si surface is expressed here in units of a monolayer (ML) on a Si(111) crystalline surface; 1-ML Sb corresponds to 7.8×10^{14} atoms/cm^2. The resulting films were characterized by transmission-electron microscopy (TEM) and diffraction (TED) and *in situ* reflection high-energy electron diffraction (RHEED).

First, we report the experimental results of Si-MBD on clean *a*-Si surfaces without the Sb surfactant. Figures 1(a) and 1(b) show cross-sectional high-resolution (HR) TEM images of samples grown by Si-MBD at 550 °C for 410 and 100 s, respectively. It is observed in Fig. 1(a) that a polycrystalline-Si (poly-Si) layer was formed on the predeposited *a*-Si layer. The polycrystalline structure was also observed during deposition by *in situ* RHEED, showing a ring pattern. Figure 1(b) illustrates an intermediate state of the formation of the poly-Si/*a*-Si structure shown in Fig. 1(a). It should be noted that the grain on the *a*-Si layer grows in a hemispherical shape. Furthermore, concave surface morphology of the *a*-Si can be seen around the grain, as indicated by arrow heads. Such depletion of the *a*-Si layer can also be observed in Fig. 1(a).

This poly-Si/*a*-Si structure is expected from our previous studies in which short period (5–30 s) Si-MBD resulted in the formation of Si microcrystals on the *a*-Si surface.[14] When we continued Si-MBD for longer periods, as in the present case, the microcrystals on the surface grow larger in two ways: outward growth due to the Si molecular-beam flux and inward growth due to solid-phase epitaxy into the predeposited *a*-Si layer. Thus the film structure is eventually determined by the kinetics of these two growth modes. With the substrate tempera-

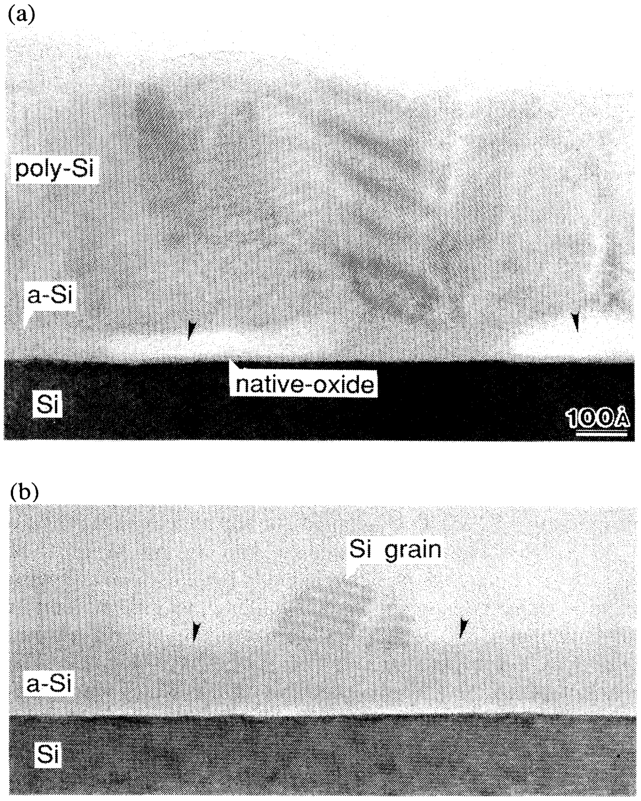

FIG. 1. Cross-sectional HR TEM micrographs of samples grown by Si-MBD on a-Si substrates at 550 °C for 410 (a) and 100 s (b). Arrow heads in each micrograph show the depletion of the a-Si layer.

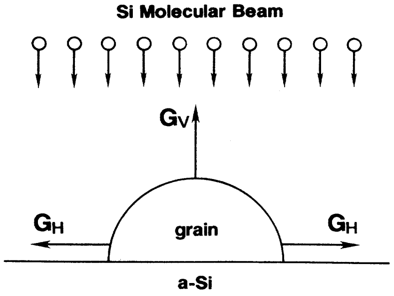

FIG. 2. Schematic illustration of the surface hemispherical grain growth modes. The arrows G_V and G_H show the growth rates in the vertical and horizontal directions, respectively.

tures and the flux density of the Si molecular beam used in the present experiments, the outward growth of the grain is much faster than the inward growth. Furthermore, the number density of the grain is increased by longer deposition times.[14] Consequently, the grains coalesce forming a polycrystalline texture on the a-Si surface.

From these results, we can also deduce the atomistic process of the grain growth, i.e., crystallization of the Si adatoms on the clean a-Si surface during Si-MBD. Define the vertical (G_V) and horizontal (G_H) growth rates of the surface hemispherical grain under the Si molecular-beam flux as shown in Fig. 2. One of the factors which determines the value of each growth rate is the orientation of the Si molecular beam with respect to the grain. The Si molecular beam has high unidirectionality. Thus, in the present geometry, G_H is much less than G_V since the beam flux can increase only the G_V value. The fact that isotropic growth of the hemispherical grain was, nevertheless, observed requires another factor to result in G_H and G_V being approximately the same. One can easily deduce that this is due to diffusion of the Si adatoms on the surface during deposition. Diffusion of adatoms on the clean surfaces of crystalline Si substrates in MBE has been exhaustively reported[15] and it was recently observed that the surface atoms of a-Si with a clean, native oxide-free surface were also diffusive enough to crystallize on that surface.[16,17] Diffusion of the Si adatoms is also supported by the depletion of the a-Si layer around the grain observed in Fig. 1, indicating transport of the atoms from the a-Si matrix to the grain during grain growth. We, therefore, believe that G_H is mainly due to the atomic flux caused by diffusion of Si adatoms on both the a-Si and the grain surfaces.

Next, we report on surfactant-mediated Si-MBD. Surprisingly, adsorbing Sb on the predeposited a-Si surface prior to Si-MBD results in amorphous films rather than crystalline grains, even though all other growth conditions are the same as above. Figure 3 shows a typical cross-sectional HR TEM image of a sample formed by Si-MBD at 550 °C for 410 s on a 1.7-ML Sb-absorbed surface. All regions of the deposited film have a mottled contrast indicating amorphous structure and the plan-view TED pattern shows a diffuse ring which is also characteristic of amorphous materials. A wide range of TEM observations showed no crystalline phases in the films. This amorphous structure was also confirmed by *in situ* RHEED during deposition.

The sample shown in Fig. 3 was also investigated by *in situ* AES observations. The spectrum for the Sb-adsorbed a-Si surface just before Si-MBD showed Si and

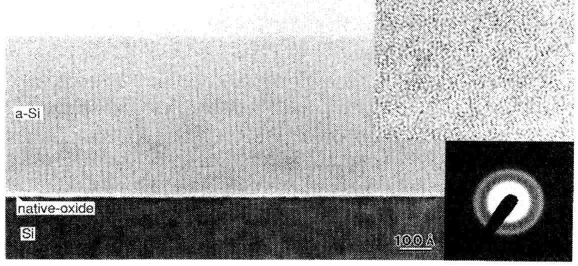

FIG. 3. Cross-sectional HR TEM micrograph of a sample showing amorphous structure grown by Si-MBD at 550 °C for 410 s on a Sb-adsorbed a-Si substrate. Insets are a larger magnification image of the deposited film showing mottled contrast and a plan-view TED pattern taken from the film showing a diffuse ring.

Sb peaks of 92 and 454 eV, respectively. The Sb peak corresponding to 1 ML in amount could be observed even after Si-MBD for 410 s on that surface. Since the escape depth of the Sb Auger electron (about 10 Å) is short compared with the thickness of the deposited *a*-Si layer (about 400 Å), the peak is truly from the surface of the deposited film. This result means that the adsorbed Sb segregates to the surface during Si-MBD. This behavior of the Sb segregation is quite similar to the cases of surfactant-mediated epitaxy[2,5–7] and Si-MBE on Sb-terminated Si crystalline surfaces.[18,19] We expect that the surface-free energy of the Sb-Si system in the amorphous phase is nearly identical to that of the Sb-Si crystalline systems. This is because although the long-range order is different, the local atomic structure is the same in both systems; e.g., covalency of the chemical bonds and atomic coordination number.[20–22] Therefore, it seems likely that thermodynamics based on the surface energy reduction of the Si surface by the surfactant[1,2,18] may also be employed to explain the rapid incorporation of Si adatoms into subsurface sites of *a*-Si.

To this point we have demonstrated that Sb surfactant prevents the crystallization of Si adatoms on the *a*-Si surface. In order to understand in detail the atomistic process of this phenomenon, further experiments were performed. First, Si microcrystals were formed on clean *a*-Si surfaces by our seeding method[14] and subsequently 1–2-ML Sb was evaporated onto the seeded *a*-Si surfaces. Si-MBD was then conducted on that surface. Figure 4 shows plan-view (a) and cross-sectional (b) TEM images of a sample in which each growth step was performed at 550 °C. Note that crystalline phases having columnar structures are embedded in the amorphous matrix. Furthermore, we observed that the number densities of the columnar grains and the original seeded grains are almost identical ($\sim 2\times10^{10}/\mathrm{cm}^2$). Consequently, it is reasonable to interpret that the columnar grains were grown from the seeded grains during Si-MBD while the amorphous phase was formed on the rest of the surface. In analogy to the grain growth kinetics of the nonsurfactant case mentioned above, the columnar structure of the grain is attributed to the fact that G_H is much less than G_V during the growth process. Since G_H is primarily determined by the atomic flux due to surface diffusion of the Si adatoms, the lower value of G_H directly indicates a shorter diffusion length for Si adatoms on the surfactant-terminated surface. We, therefore, conclude that during Si-MBD the Si adatoms deposited on the Sb-terminated surface are incorporated into an *a*-Si subsurface site after diffusing only a short distance.

Nucleation of Si adatoms on the *a*-Si surface is a principal process in the initial stage of crystallization. Rapid incorporation into the subsurface and the short diffusion length sharply reduce the concentration of the surface-free adatoms, giving rise to a drastic decrease in the nucleation rate on the surface. In this manner, nucleation of Si adatoms is prevented throughout deposition, so that the resulting film has a disordered structure similar to the *a*-Si substrate.

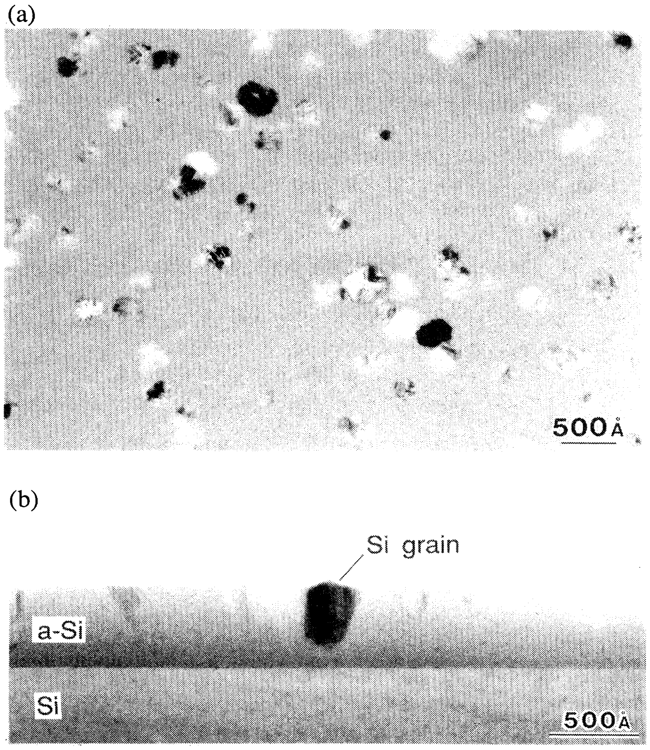

FIG. 4. Plan-view (a) and cross-sectional (b) TEM micrographs of a sample showing the columnar structure of Si grains embedded in an *a*-Si matrix.

In summary, the effect of Sb surfactant on the crystallization of Si adatoms on the *a*-Si surface was investigated. We observed that the adsorbed Sb segregated to the surface during Si-MBD and prevented crystallization, giving rise to *a*-Si formation even at medium temperatures. Reduction by the surfactant of the diffusion length of the surface-free adatoms was confirmed by comparison of grain growth modes on *a*-Si surfaces with and without the surfactant.

The authors would like to thank D. Tweet and N. Ikarashi for their valuable discussions and M. Oshida for her helpful assistance in the experiments. Thanks are also due to Y. Matsumoto and H. Watanabe for their encouragement.

---

[1] M. Copel, M. C. Reuter, E. Kaxiras, and R. M. Tromp, Phys. Rev. Lett. **63**, 632 (1989).

[2] M. Copel, M. C. Reuter, M. Horn von Hoegen, and R. M. Tromp, Phys. Rev. B **42**, 11 682 (1990).

[3] F. K. LeGoues, M. Copel, and R. M. Tromp, Phys. Rev. Lett. **63**, 1826 (1989).

[4] F. K. LeGoues, M. Copel, and R. M. Tromp, Phys. Rev. B **42**, 11 690 (1990).

[5] M. Horn von Hoegen, F. K. LeGoues, M. Copel, M. C. Reuter, and R. M. Tromp, Phys. Rev. Lett. **67**, 1130 (1991).

[6] J. M. C. Thornton, A. A. Williams, J. E. Macdonald, R. G. van Silfhout, M. S. Finney, and C. Norris, Surf. Sci. **273**, 1 (1992).

[7] H. J. Osten, J. Klatt, G. Lippert, E. Bugiel, and S. Hinrich, Appl. Phys. Lett. **60**, 2522 (1992).

[8] H. J. Osten, J. Klatt, G. Lippert, B. Dietrich, and E. Bugiel, Phys. Rev. Lett. **69**, 450 (1992).

[9] H. A. van der Vegt, H. M. van Pinxteren, M. Lohmeier, E. Vlieg, and J. M. C. Thornton, Phys. Rev. Lett. **68**, 3335 (1992).

[10] R. M. Tromp and M. C. Reuter, Phys. Rev. Lett. **68**, 954 (1992).

[11] H. Ishiwara, H. Yamamoto, S. Furukawa, M. Tamura, and T. Tokuyama, Appl. Phys. Lett. **43**, 1028 (1983).

[12] G. L. Olson and J. A. Roth, Mater. Sci. Rep. **3**, 1 (1988).

[13] M. Matsui, Y. Shiraki, Y. Katayama, K. L. I. Kobayashi, A. Shintani, and E. Maruyama, Appl. Phys. Lett. **37**, 936 (1980).

[14] A. Sakai and T. Tatsumi, Appl. Phys. Lett. **61**, 159 (1992).

[15] For example, Y.-W. Mo, J. Kleiner, M. B. Webb, and M. G. Laggally, Phys. Rev. Lett. **66**, 1998 (1991).

[16] A. Sakai, H. Ono, K. Ishida, T. Niino, and T. Tatsumi, Jpn. J. Appl. Phys. **30**, L941 (1991).

[17] A. Sakai, T. Tatsumi, Taeko Niino, Haruhiko Ono, and K. Ishida, Denki Kagaku **50**, 1043 (1991).

[18] H. Jorke, Surf. Sci. **193**, 569 (1988).

[19] R. A. Metzger and F. G. Allen, J. Appl. Phys. **55**, 931 (1984).

[20] D. E. Polk and D. S. Boudreaux, Phys. Rev. Lett. **31**, 92 (1973).

[21] F. Wooten, K. Winer, and D. Weaire, Phys. Rev. Lett. **54**, 1392 (1985).

[22] R. Car and M. Parrinello, Phys. Rev. Lett. **60**, 204 (1988).

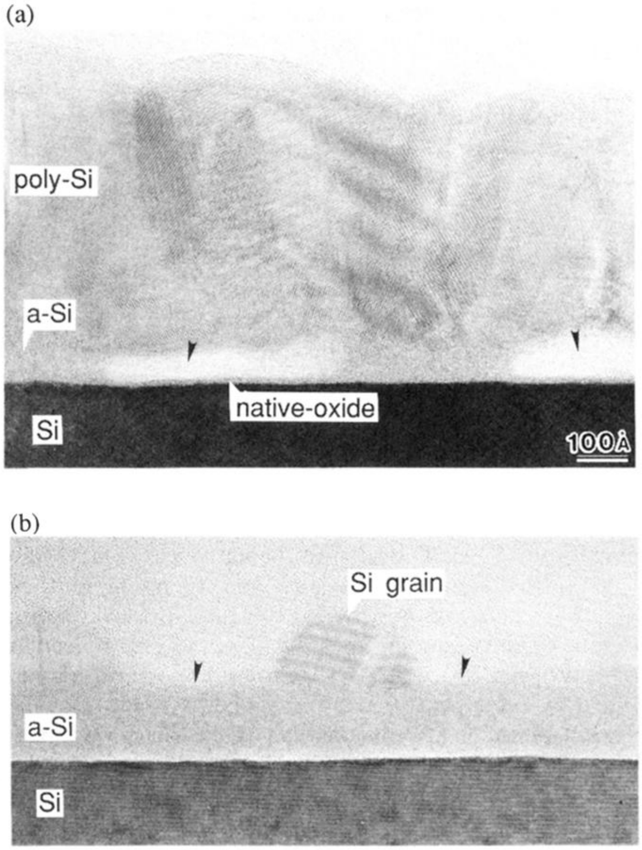

FIG. 1. Cross-sectional HR TEM micrographs of samples grown by Si-MBD on *a*-Si substrates at 550 °C for 410 (a) and 100 s (b). Arrow heads in each micrograph show the depletion of the *a*-Si layer.

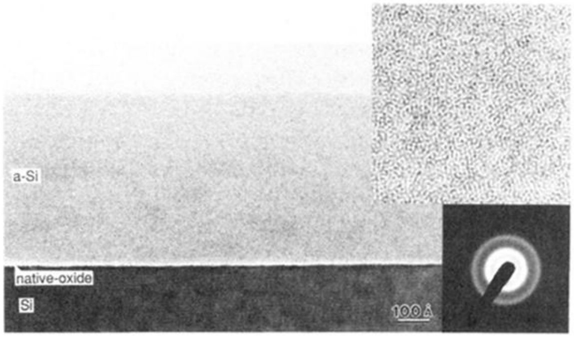

FIG. 3. Cross-sectional HR TEM micrograph of a sample showing amorphous structure grown by Si-MBD at 550 °C for 410 s on a Sb-adsorbed *a*-Si substrate. Insets are a larger magnification image of the deposited film showing mottled contrast and a plan-view TED pattern taken from the film showing a diffuse ring.

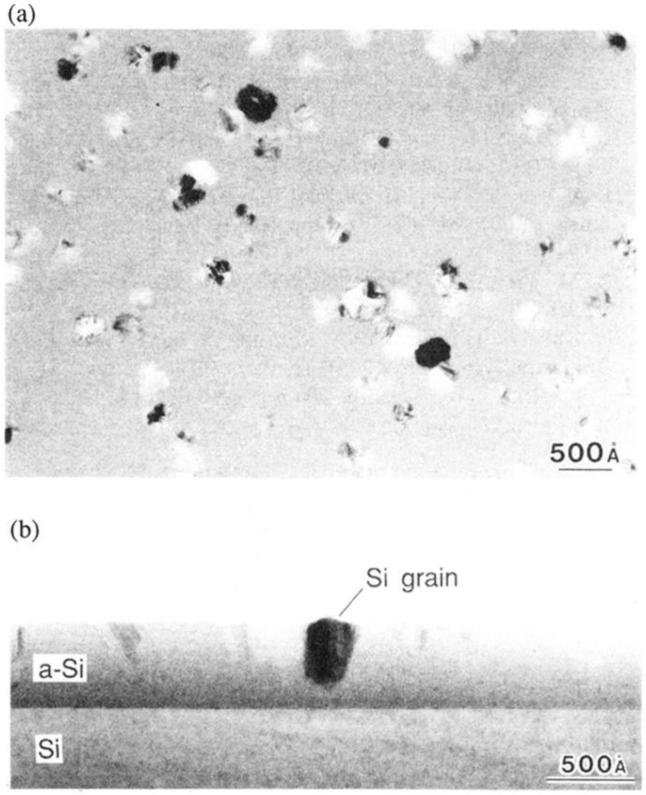

FIG. 4. Plan-view (a) and cross-sectional (b) TEM micrographs of a sample showing the columnar structure of Si grains embedded in an *a*-Si matrix.